chromatography [24]. The level of DNA adduct formation was defined as the relative adduct level (RAL) which was determined by calculating the level of radioactivity in the adduct nucleotides per (radioactivity in total nucleotides × dilution factor). After 4 weeks' exposure to the urban air, the RAL of total DNA adducts in the lung and of the major DNA adduct in the liver increased from control levels of $0.8/10^8$ and $1.3/10^8$ nucleotides to $13.1/10^8$ and $6.6/10^8$ nucleotides, respectively [23]. However, the RAL in the lung decreased to a steady level of around $3/10^8$ nucleotides after prolonged exposure for over 12 weeks. This decrease was also observed in the liver, thus suggesting that prolonged exposure to air pollution activates the DNA repair system.

After *in situ* exposure of rats for 24 h to coke oven emissions, which contain carcinogenic PAHs and BaP at 892 and 118 ng/m^3, respectively, DNA adduct formation was induced in the lung and in extrapulmonary tissues [25]. The RAL of total DNA adducts was about $4.8/10^8$ nucleotides in both the liver and lung, but was lower at about $0.8/10^8$ nucleotides in white blood cells (WBCs). By comparison, the RAL of the BaP–DNA adduct, the major DNA adduct induced, was elevated to $1.6/10^8$ nucleotides in the lung, $1.3/10^8$ in the heart, and $0.5/10^8$ in WBCs compared with control rats ($0.3/10^8$ nucleotides in the lung, $0.2/10^8$ in the liver, and $0.2/10^8$ in WBCs). DNA adduct formation in rat liver and kidney was also observed after a single intratracheal administration of 3NBA [15]. Pollutants, such as PAHs and nitro-PAHs, absorbed into the lung have been shown to be systemically transported from the lung to other organs [15, 23, 25], but the mechanism underlying their movement to other organs remains unknown.

An *in situ* exposure study to estimate the mutagenicity of urban air was conducted in Hamilton Harbor, Ontario, Canada [26]. In this study, mice were housed near steel mills and a major highway, and were exposed *in situ* to ambient air containing a mean of 93.8 $\mu g/m^3$ total suspended particles and 8.3 ng/m^3 PAHs [26]. The RAL of DNA adducts in the lung was significantly higher after 3 weeks' exposure ($1/10^8$ nucleotides) compared with control mice breathing HEPA-filtered air ($0.7/10^8$ nucleotides). Prolonged exposure to the ambient air for 10 weeks, followed by maintenance of animals in the laboratory for 6 weeks, induced 1.58-fold increase in sperm mutation frequency of expanded simple tandem repeat compared with the control mice.

Observations by *in situ* exposure studies suggest that mutagenic compounds, such as PAHs and nitro-PAHs, in SPM in urban air can produce DNA adducts that cause gene mutations.

3. DNA Adduct Formation and *In Vivo* Mutagenesis by Exposure to Diesel Exhaust

Methods for detecting the genotoxicity of xenobiotics in somatic cells include the micronuclear test and the chromosomal aberration assay [27]. A comprehensive method for assessing mutations in somatic cells and germ cells is the transgenic rodent mutation assay, which can detect and quantify mutations, including base substitutions, deletions, and insertions [28]. In the assay, multiple copies of a target gene (*E. coli* gene) carried on a shuttle vector are integrated into genomic DNA. Four types of transgenic rodent models have

been developed: the Muta mouse, the Big Blue mouse and rat, the *gpt* delta mouse and rat, and the *rpsL* gene transgenic mouse model. In the Muta mouse, the *lacZ* gene, encoding beta-galactosidase, on a lambda phage is integrated into the genomic DNA. The Big Blue mouse and rat are based on the integration into the genome of the *lacI* (*lac* operon repressor) gene on a lambda phage. Transgenic medaka fish (*Oryzias latipes*) have also been generated with *lacI* gene on a lambda phage for monitoring of mutagens in aquatic environment [29]. The *gpt* delta transgenic mouse and rat [30] have the *gpt* gene, encoding guanine phosphoribosyl transferase, integrated into the genome. In this model, large DNA deletions are detectable using the *red/gam* gene located on the lambda phage [31]. In the *rpsL* gene transgenic mouse model, *rpsL*, which confers streptomycin sensitivity in *E. coli*, is the mutational target gene and is integrated into the mouse genome on a plasmid [32]. Transgenic zebrafish harboring *rpsL* have also been generated for mutation studies [33]. The target genes that have integrated into the genomic DNA of the transgenic model animals are rescued to *E. coli* by transfection; the mutated target gene is then detected by positive selection (or negative selection for *lacZ* mutation assay) of transfected *E. coli*. Mutant frequency (MF) is defined as number of mutant colonies or plaques per titer. Sequence analysis of mutated target genes can detect and quantify the types of mutations.

To assess the DNA adduct-producing potency of SPM and its relationship to *in vivo* mutagenicity, Big Blue rats were exposed to diesel engine exhaust (DE), a major source of SPM in urban areas and a model air pollutant [14]. After continuous inhalation by the rats of DE at either 1 or 6 mg SPM/m^3 for 4 weeks, the RAL of DNA adducts was $23/10^8$ and $48/10^8$ nucleotides, respectively. The inhalation of 6 mg SPM/m^3 DE gave a significant ($P<0.01$) elevation of MF: 4.25×10^{-5} in lung exposed to DE compared with 0.88×10^{-5} in control lung. By comparison, inhalation of 1 mg SPM/m^3 did not cause a significant increase in MF. Although the concentration of SPM in DE at 6 mg/m^3 is over 78 times the concentration (76.5 µg/m^3) found in urban air, some of which may originate from DE, the DNA adduct level induced by DE inhalation was only 3.7 times higher than that induced by urban air ($13.1/10^8$) over the same period (4 weeks) of exposure [23]. This observation may be explained by a non-linear (saturated) dose response between the level of exposure and DNA adduct at high dose, which was demonstrated in rat lung exposed to a coal-tar pitch aerosol [34].

Increase in MF by inhalation of DE was also shown in the lung of *gpt* delta mice [35]. After continuous inhalation of DE at 3 mg SPM/m^3 for 4 weeks, the MF in the lung elevated to significantly higher levels (1.06×10^{-5}) than in the control lung (0.61×10^{-5}) ($P<0.05$). The DNA adduct level was not determined in the lungs of *gpt* delta mice exposed to DE, but was determined in a separate experiment under the same conditions of DE exposure: the RAL of DNA adducts increased to $11/10^8$ nucleotides ($3/10^8$ nucleotides in the control) [36]. By comparison, a higher concentration of DE (20 mg SPM/m^3) and a shorter exposure period (a single 90-min exposure period on each of four consecutive days) resulted in a slight but significant increase in DNA adduct formation in the lung of the Muta mouse 1 h after the last exposure period [37]. Under these conditions, the MF in the lung was not elevated [37].

The mutagenic and DNA adduct-forming potencies of PAH and nitro-PAH in the lung were examined by a single intratracheal administration. Intratracheal administration of 10 mg BaP/animal (30–40 mg/body weight) in Big Blue rats induced a doubling in the MF from the

control level of 3.1 × 10^{-5} to 6.1 × 10^{-5} at 4 weeks after dosing [38], while the RAL in BaP-treated lungs was $5.1/10^8$ nucleotides. BaP administration induced a lower RAL in the lung than did DE inhalation, but the increase in MF was similar in both treatments [14,38]. Intratracheal administration of 1 mg BaP (about 40 mg/body weight) increased the MF in *gpt* delta mouse lungs to 2.52 × 10^{-5} from the control MF of 0.60 × 10^{-5} [13]. The mutagenic potency of BaP in lungs is similar in rats and mice when the BaP dose is normalized to body weight. In the lungs of *gpt* delta mice, 1,6-DNP gave a markedly higher MF of 31 × 10^{-5} per mg [12] than that of BaP at 1.7 × 10^{-5} per mg [13]. The type of mutations induced by DE, BaP, and 1,6-DNP were assessed. The G:C→A:T transition was the major base substitution induced by DE in the lungs of Big Blue rats [14] and *gpt* delta mice [35]. By comparison, BaP and 1,6-DNP tended to induce G:C→T:A transversions and G:C→A:T transitions, respectively [12, 13]. Interestingly, the mutation hot spots induced by DE inhalation were similar to those induced by 1,6-DNP (Fig. 1), but these sites were different from those induced by BaP [13]. These results suggest that DNPs and related compounds are the major mutagens in DE.

In the transgenic rodent study, the RAL for DNA adducts of $>5/10^8$ nucleotides, which was produced by intratracheal administration of BaP [38], possibly gave a markedly increase in the MF in the lung. Exposure of V79 cells to the BaP metabolite BPDE revealed that the MF of the *HPRT* gene and the RAL for DNA adducts gave a concentration-dependent linear increase with an MF-to-RAL ratio of 4.39 × 10^{-9} [39]. However, it was unclear how the levels of DNA adduct formation (RAL) induced by the mutagen were quantitatively related to *in vivo* mutagenicity.
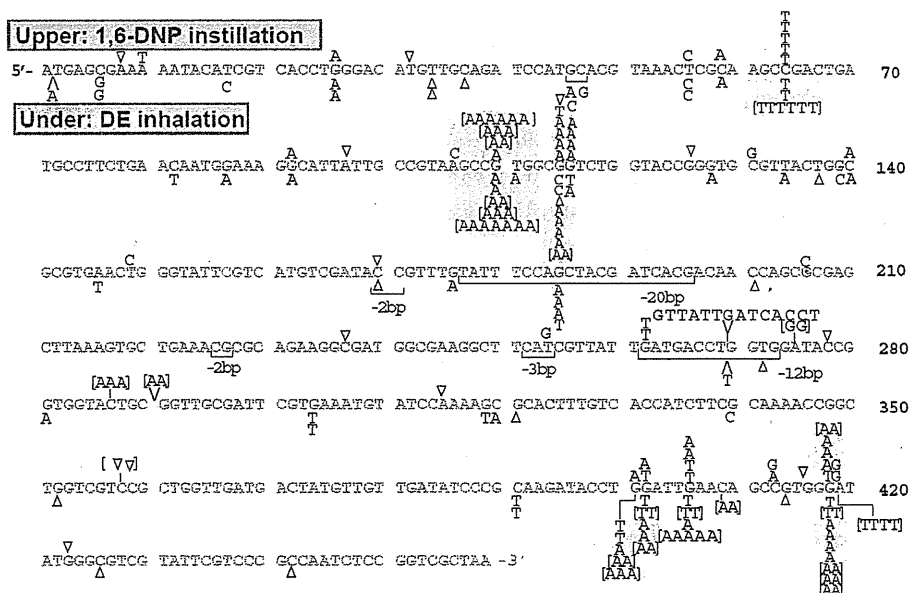

Figure 1. Overall distribution of the mutations detected in the *gpt* gene in the lungs of mice treated with 1,6-DNP by intratracheal administration and those treated with DE by inhalation exposure. The mutations induced by 1,6-DNP [12] and DE [35] are shown, respectively, above and below the *gpt* sequence. The number of characters in parentheses is the number of mutations in one mouse. Δ, one base deletion; half-boxes, deleted nucleotides; V, a position of insertion.

4. DNA Adduct Formation in Humans

DNA adducts are useful biomarkers for monitoring exposure to PAHs and may be useful for assessing the potential mutagenicity of environmental pollutants. Blood cells are appropriate for detecting DNA adducts induced as a consequence of PAH exposure, and have been used in epidemiological studies in Poland, Italy, Denmark, Greece, several other European countries, and Thailand [40]. These studies revealed that the level of DNA adduct formation is higher in areas exposed to more PAHs than in areas exposed to less PAHs. Since blood cells are rapidly turned over, analysis of DNA adduct formation in human lung autopic samples have been tried, despite sampling difficulties, for monitoring long-term exposure to PAHs in ambient air. The ^{32}P-postlabeling assay showed that the total RAL for smokers was 1.5–34.3/10^8 nucleotides, whereas that for non-smokers was 1.9–3.3/10^8 nucleotides [41]. Lewtas et al. revealed that the average RAL in autopic samples was 9.42 (range, 8.34–11.1)/10^8 nucleotides in smokers and 3.15 (1.49–4.80)/10^8 nucleotides in nonsmokers [42]. The RALs for DNA adducts were also analyzed in biopsy samples of bronchial tissue and were found to be 3.45 ± 1.62/10^8 in nonsmokers, 3.93 ± 1.92/10^8 in former smokers, and 5.53 ± 2.13/10^8 in smokers [43]. In a study in Florence, Italy, the level of BPDE–DNA adducts was measured by high-performance liquid chromatography / synchronous fluorescence in autopic samples from individuals exposed to air in which PAHs were monitored [44]. The average level of total adducts was 1.76 ± 1.69/10^8 nucleotides in nonsmokers, 4.04 ± 2.37/10^8 nucleotides in ex-smokers, and 4.46 ± 5.76/10^8 nucleotides in smokers. Furthermore, the total BPDE–DNA adduct level correlated positively with the BaP level in the lung. In this study, the level of PAHs in air was 15–35 ng/m^3. In the Florence area, analysis of the relationship between the DNA adduct level in leukocytes and exposure to SPM < 10 μm in diameter (PM$_{10}$) revealed that the DNA adduct levels in nonsmoking workers reflected the level of PM$_{10}$ exposure in high traffic urban area from 1993 to 1998 [45].

5. Conclusion

As described in Section 4, the level of DNA adducts in the lungs of nonsmokers was estimated to be 1.9–3.3/10^8 nucleotides [41], which is lower than the maximum level in the lungs of rats exposed to urban air, but marginal to the steady level (around 3/10^8 nucleotides). These results demonstrate that inhalation by experimental animals can accurately reflect the impact of air pollutants in human lungs, and thus provides a useful tool for monitoring the total impact of air pollutants (e.g., DNA adduct formation by PAHs in the air). Recently, *in vivo* mutation data has been analyzed for informing the cancer risk assessment process [46]. However, further studies are required for evaluating the relationship between the DNA adduct level and *in vivo* mutagenicity by *in situ* exposure to urban air or a model pollutant, and the relationship between the *in vivo* mutagenicity and carcinogenicity for quantitative health risk assessments, especially for the risk of lung cancer from air pollution.

Acknowledgments

References

[1] International Agency for Research on Cancer. (1983) Benzo[a]pyrene. *Monogr Eval Carcinog Risk Chem Hum. 32,* 211-224.

[2] International Agency for Research on Cancer. Air Pollution, Part 1, Some Non-heterocyclic Polycyclic Aromatic Hydrocarbons and Some Related Industrial Exposures. *Monogr Eval Carcinog Risk Chem Hum. 92* in preparation. (http://monographs.iarc.fr/ENG/Classification/crthgr01.php)

[3] World Health Organization Regional Office for Europe. Air Quality Guidelines for Europe, 2nd ed.. WHO Regional Publications, European Series, No. 91. Copenhagen: World Health Organization; 2000.

[4] Integrated Risk Information System. http://www.epa.gov/NCEA/iris/subst/0136.htm. United States Environmental Protection Agency.

[5] DIRECTIVE 2004/107/EC OF THE EUROPEAN PARLIAMENT AND OF THE COUNCIL of 15 December 2004 relating to arsenic, cadmium, mercury, nickel and polycyclic aromatic hydrocarbons in ambient air. 26.1.2005, L23/3-16.

[6] Pufulete M, Battershill J, Boobis A, & Fielder R. (2004) Approaches to carcinogenic risk assessment for polycyclic aromatic hydrocarbons: a UK perspective. *Regul Toxicol Pharmacol. 40,* 54-66.

[7] World Health Organization. Environmental Health Criteria 202; Selected Non-heterocyclic Polycyclic Aromatic Hydrocarbons. Geneva: International Programme on Chemical Safety; 1998.

[8] The Ministry of the Environment, Japan. http://www.env.go.jp/air/osen/monitoring/mon_h19/tab9.html (in Japanese)

[9] World Health Organization. Environmental Health Criteria 229; Selected Nitro- and Nitro-oxy-polycyclic Aromatic Hydrocarbons. Geneva: International Programme on Chemical Safety; 2003.

[10] Takayama S, Ishikawa T, Nakajima H, & Sato S. (1985) Lung carcinoma induction in Syrian golden hamsters by intratracheal instillation of 1,6-dinitropyrene. *Jpn J Cancer Res. 76,* 457-461.

[11] Iwagawa M, Maeda T, Izumi K, Otsuka H, Nishifuji K, Ohnishi & Y, Aoki S. (1989) Comparative dose-response study on the pulmonary carcinogenicity of 1,6-dinitropyrene and benzo[a]pyrene in F344 rats. *Carcinogenesis. 10,* 1285-1290.

[12] Hashimoto AH, Amanuma K, Hiyoshi K, Takano H, Masumura K, Nohmi T, & Aoki. Y. (2006) In vivo mutagenesis in the lungs of gpt-delta transgenic mice treated intratracheally with 1,6-dinitropyrene. *Environ Mol Mutagen. 47,* 277-283.

[13] Hashimoto AH, Amanuma K, Hiyoshi K, Takano H, Masumura K, Nohmi T, & Aoki Y. (2005) In vivo mutagenesis induced by benzo[a]pyrene instilled into the lung of gpt delta transgenic mice. *Environ Mol Mutagen. 45*, 365-373.

[14] Sato H, Sone H, Sagai M, Suzuki KT, & Aoki Y. (2000) Increase in mutation frequency in lung of Big Blue rat by exposure to diesel exhaust. *Carcinogenesis. 21*, 653-661.

[15] Arlt VM. (2005) 3-Nitrobenzanthrone, a potential human cancer hazard in diesel exhaust and urban air pollution: a review of the evidence. *Mutagenesis. 20*, 399-410.

[16] Nagy E, Zeisig M, Kawamura K, Hisamatsu Y, Sugeta A, Adachi S, & Möller L. (2005) DNA adduct and tumor formations in rats after intratracheal administration of the urban air pollutant 3-nitrobenzanthrone. *Carcinogenesis. 26*, 1821-1828.

[17] Watanabe T, Hasei T, Takahashi T, Asanoma M, Murahashi T, Hirayama T, & Wakabayashi K. (2005) Detection of a novel mutagen, 3,6-dinitrobenzo[e]pyrene, as a major contaminant in surface soil in Osaka and Aichi Prefectures, Japan. *Chem Res Toxicol. 18*, 283-289.

[18] Watanabe T, Takahashi K, Konishi E, Hoshino Y, Hasei T, Asanoma M, Hirayama T, & Wakabayashi K. (2008) Mutagenicity of surface soil from residential areas in Kyoto city, Japan, and identification of major mutagens. *Mutat Res. 649*, 201-212.

[19] Nebert DW, & Negishi M. (1982) Multiple forms of cytochrome P-450 and the importance of molecular biology and evolution. *Biochem Pharmacol. 31*, 2311-2317.

[20] Miller EC, & Miller JA. (1981) Mechanisms of chemical carcinogenesis. *Cancer. 47(5 Suppl)*, 1055-1064.

[21] Harris CC. (1985) Future directions in the use of DNA adducts as internal dosimeters for monitoring human exposure to environmental mutagens and carcinogens. *Environ Health Perspect. 62*, 185-91.

[22] Bailleul B, Brown K, Ramsden M, Akhurst RJ, Fee F, & Balmain A. (1989) Chemical induction of oncogene mutations and growth factor activity in mouse skin carcinogenesis. *Environ Health Perspect. 81*, 23-27.

[23] Sato H, Suzuki KT, Sone H, Yamano Y, Kagawa J, & Aoki Y. (2003) DNA-adduct formation in lungs, nasal mucosa, and livers of rats exposed to urban roadside air in Kawasaki City, Japan. *Environ Res. 93*, 36-44.

[24] Reddy MV, & Randerath K. (1986) Nuclease P1-mediated enhancement of sensitivity of 32P-postlabeling test for structurally diverse DNA adducts. *Carcinogenesis. 7*, 1543-51.

[25] Binková B, Dobiás L, Wolff T, & Srám RJ. (1994) 32P-postlabeling analysis of DNA adducts in tissues of rats exposed to coke-oven emissions. *Mutat Res. 307*, 355-63.

[26] Yauk C, Polyzos A, Rowan-Carroll A, Somers CM, Godschalk RW, Van Schooten FJ, Berndt ML, Pogribny IP, Koturbash I, Williams A, Douglas GR, & Kovalchuk O. (2008) Germ-line mutations, DNA damage, and global hypermethylation in mice exposed to particulate air pollution in an urban/industrial location. *Proc Natl Acad Sci USA. 105*, 605-10.

[27] World Health Organization. Environmental Health Criteria 51; Guide to Short-term Tests for Detecting Mutagenic and Carcinogenic Chemicals. Geneva: International Programme on Chemical Safety; 2003.

[28] Lambert IB, Singer TM, Boucher SE, & Douglas GR. (2005) Detailed review of transgenic rodent mutation assays. *Mutat Res. 590*, 1-280.

[29] Winn RN, Norris MB, Brayer KJ, Torres C, & Muller SL. (2000) Detection of mutations in transgenic fish carrying a bacteriophage lambda cII transgene target. *Proc Natl Acad Sci USA. 97*, 12655-12660.

[30] Hayashi H, Kondo H, Masumura K, Shindo Y, & Nohmi T. (2003) Novel transgenic rat for in vivo genotoxicity assays using 6-thioguanine and Spi- selection. *Environ Mol Mutagen. 41*, 253-259.

[31] Nohmi T, Katoh M, Suzuki H, Matsui M, Yamada M, Watanabe M, Suzuki M, Horiya N, Ueda O, Shibuya T, Ikeda H, & Sofuni T. (1996) A new transgenic mouse mutagenesis test system using Spi- and 6-thioguanine selections. *Environ Mol Mutagen. 28*, 465-470.

[32] Gondo Y, Shioyama Y, Nakao K, & Katsuki M. (1996) A novel positive detection system of in vivo mutations in rpsL (strA) transgenic mice. *Mutat Res. 360*, 1-14.

[33] Amanuma K, Takeda H, Amanuma H, & Aoki Y. (2000) Transgenic zebrafish for detecting mutations caused by compounds in aquatic environments. *Nat Biotechnol. 18*, 62-65.

[34] Lewtas J, Walsh D, Williams R, & Dobiás L. (1997) Air pollution exposure-DNA adduct dosimetry in humans and rodents: evidence for non-linearity at high doses. *Mutat Res. 378*, 51-63.

[35] Hashimoto AH, Amanuma K, Hiyoshi K, Sugawara Y, Goto S, Yanagisawa R, Takano H, Masumura K, Nohmi T, & Aoki Y. (2007) Mutations in the lungs of gpt delta transgenic mice following inhalation of diesel exhaust. *Environ Mol Mutagen. 48*, 682-693.

[36] Aoki Y, Sato H, Nishimura N, Takahashi S, Itoh K, & Yamamoto M. (2001) Accelerated DNA adduct formation in the lung of the Nrf2 knockout mouse exposed to diesel exhaust. *Toxicol Appl Pharmacol. 173*, 154-160.

[37] Dybdahl M, Risom L, Bornholdt J, Autrup H, Loft S, & Wallin H. (2004) Inflammatory and genotoxic effects of diesel particles in vitro and in vivo. *Mutat Res. 562*, 119-131.

[38] Loli P, Topinka J, Georgiadis P, Dusinská M, Hurbánková M, Kovácikova Z, Volkovová K, Wolff T, Oesterle D, & Kyrtopoulos SA. (2004) Benzo[a]pyrene-enhanced mutagenesis by asbestos in the lung of lambda-lacI transgenic rats. *Mutat Res. 553*, 79-90.

[39] Helleberg H, Xu H, Ehrenberg L, Hemminki K, Rannug U, & Törnqvist M. (2001) Studies of dose distribution, premutagenic events and mutation frequencies for benzo[a]pyrene aiming at low dose cancer risk estimation. *Mutagenesis. 16*, 333-337.

[40] Vineis P, & Husgafvel-Pursiainen K. (2005) Air pollution and cancer: biomarker studies in human populations. *Carcinogenesis. 26*, 1846-1855.

[41] Phillips DH, Hewer A, Martin CN, Garner RC, & King MM. (1988) Correlation of DNA adduct levels in human lung with cigarette smoking. *Nature. 336*, 790-792.

[42] Lewtas J, Mumford J, Everson RB, Hulka B, Wilcosky T, Kozumbo W, Thompson C, George M, Dobiás L, Srám R, Xueming L, & Gallagher J. (1993) Comparison of DNA adducts from exposure to complex mixtures in various human tissues and experimental systems. *Environ Health Perspect. 99*, 89-97.

[43] Phillips DH, Schoket B, Hewer A, Bailey E, Kostic S, & Vincze I. (1990) Influence of cigarette smoking on the levels of DNA adducts in human bronchial epithelium and white blood cells. *Int J Cancer. 46*, 569-575.

[44] Lodovici M, Akpan V, Giovannini L, Migliani F, & Dolara P. (1998) Benzo[a]pyrene diol-epoxide DNA adducts and levels of polycyclic aromatic hydrocarbons in autoptic samples from human lungs. *Chem Biol Interact. 116*, 199-212.

[45] Palli D, Saieva C, Munnia A, Peluso M, Grechi D, Zanna I, Caini S, Decarli A, Sera F, & Masala G. (2008) DNA adducts and PM10 exposure in traffic-exposed workers and urban residents from the EPIC-Florence City study. *Sci Total Environ. 403*, 105-112.

[46] Moore MM, Heflich RH, Haber LT, Allen BC, Shipp AM, & Kodell RL. (2008) Analysis of in vivo mutation data can inform cancer risk assessment. *Regul Toxicol Pharmacol. 51*, 151-161.

ORIGINAL ARTICLE

A novel protein, MAPO1, that functions in apoptosis triggered by O⁶-methylguanine mispair in DNA

K Komori[1], Y Takagi[2], M Sanada[3], T-H Lim[4], Y Nakatsu[4], T Tsuzuki[4], M Sekiguchi[1,2] and M Hidaka[1,3,4]

[1]Department of Molecular Biology, Biomolecular Engineering Research Institute, Suita, Japan; [2]Frontier Research Center, Fukuoka Dental College, Fukuoka, Japan; [3]Department of Physiological Science and Molecular Biology, Fukuoka Dental College, Fukuoka, Japan and [4]Department of Medical Biophysics and Radiation Biology, Faculty of Medical Sciences, Kyushu University, Fukuoka, Japan

O⁶-Methylguanine produced in DNA induces mutation due to its ambiguous base-pairing properties during DNA replication. To suppress such an outcome, organisms possess a mechanism to eliminate cells carrying O⁶-methylguanine by inducing apoptosis that requires the function of mismatch repair proteins. To identify other factors involved in this apoptotic process, we performed retrovirus-mediated gene-trap mutagenesis and isolated a mutant that acquired resistance to a simple alkylating agent, N-methyl-N-nitrosourea (MNU). However, it was still sensitive to methyl methanesulfonate, 1-(4-amino-2-methyl-5-pyrimidinyl)methyl-3-(2-chloroethyl)-3-nitrosourea, etoposide and ultraviolet irradiation. Moreover, the mutant exhibited an increased mutant frequency after exposure to MNU. The gene responsible was identified and designated Mapo1 (O⁶-methylguanine-induced apoptosis 1). When the expression of the gene was inhibited by small interfering RNA, MNU-induced apoptosis was significantly suppressed. In the Mapo1-defective mutant cells treated with MNU, the mitochondrial membrane depolarization and caspase-3 activation were severely suppressed, although phosphorylation of p53, CHK1 and histone H2AX was observed. The orthologs of the Mapo1 gene are present in various organisms from nematode to humans. Both mouse and human MAPO1 proteins expressed in cells localize in the cytoplasm. We therefore propose that MAPO1 may play a role in the signal-transduction pathway of apoptosis induced by O⁶-methylguanine-mispaired lesions.
Oncogene (2009) 28, 1142–1150; doi:10.1038/onc.2008.462; published online 12 January 2009

Keywords: apoptosis; gene-trap mutagenesis; Mapo1; MGMT; O⁶-methylguanine

Correspondence: Dr M Hidaka, Department of Physiological Science and Molecular Biology, Fukuoka Dental College, 2-15-1 Tamura, Sawara-ku, Fukuoka 814-0193, Japan.
E-mail: hidaka@college.fdcnet.ac.jp

Introduction

The modification of DNA bases occurs spontaneously during normal cell growth, and the rate of formation of modified bases increases considerably when cells are exposed to radiation and certain chemical agents. O⁶-methylguanine is one of such bases produced by the action of simple alkylating agents, such as N-methyl-N-nitrosourea (MNU) and N-methyl-N'-nitro-N-nitrosoguanidine (Beranek, 1990). This modified base can pair with thymine as well as cytosine during DNA replication, and a G:C to A:T transition mutation ensues after two cycles of DNA replication (Coulondre and Miller, 1977; Loechler et al., 1984; Ito et al., 1994). To prevent such outcomes, organisms possess a specific DNA repair enzyme, O⁶-methylguanine-DNA methyltransferase (MGMT), which transfers a methyl group from the O⁶-methylguanine moiety to its own molecule, thereby repairing the DNA lesion in a single-step reaction (Pegg, 2000; Margison and Santibanez-Koref, 2002; Kaina et al., 2007). $Mgmt^{-/-}$ mice, which are defective in the methyltransferase gene, are hypersensitive to the killing effect of alkylating agents and suffer from severe damage in the bone marrow and intestinal mucosa, which are largely composed of rapidly growing cells (Tsuzuki et al., 1996; Sakumi et al., 1997; Glassner et al., 1999). Studies with cell lines derived from $Mgmt^{-/-}$ mice further revealed that O⁶-methylguanine-induced cell death occurs by apoptosis, which requires at least one round of DNA replication for its induction (Tominaga et al., 1997; Meikrantz et al., 1998).

A notable feature of O⁶-methylguanine-induced apoptosis is the requirement of mismatch repair (MMR) proteins, such as MSH2 and MLH1 (Hickman and Samson, 1999; Pepponi et al., 2003). Studies with cell lines derived from human tumors revealed that the lack of some of these gene functions rendered MGMT-deficient cells resistant to alkylating agents (Branch et al., 1993; Kat et al., 1993). Recent studies with $Mgmt^{-/-} Mlh1^{-/-}$ cells, derived from gene-targeted mice, have shown that the MLH1 protein is indeed required for the execution of apoptosis triggered by O⁶-methylguanine (Kawate et al., 1998; Takagi et al., 2003). We have shown that MutSα, consisting of MSH2 and

MSH6 proteins, and PCNA bind to O^6-methylguanine-containing DNA to form an initial complex, and MutLα, composed of MLH1 and PMS2, binds to this complex (Hidaka et al., 2005). However, the precise mechanisms regarding how the MMR complex activates the apoptotic signal remain to be elucidated. Two hypotheses have so far been proposed: the MMR complex formed on chromatin might induce the apoptotic signal (Fishel, 1998) or abortive repair cycle initiated by the complex might lead to apoptosis (Karran, 2001).

The activation of ATR kinase and phosphorylation of its downstream targets have been shown to take place in an MMR protein-dependent manner in cells treated with MNU (Caporali et al., 2004; Stojic et al., 2004; Sanada et al., 2007). The MMR protein-dependent release of cytochrome c from mitochondria and activation of caspases, which are hallmarks for apoptosis, also occur in the case of O^6-methylguanine-induced apoptosis (Ochs and Kaina, 2000; Takagi et al., 2003; Hickman and Samson, 2004). As apoptosis caused by bulky DNA lesions that block DNA replication occurs even in cells deficient in MMR proteins (Peng et al., 2007; Sanada et al., 2007), the apoptosis pathway induced by O^6-methylguanine, which does not block DNA replication, appears to be distinct from the former. It is highly likely that other proteins are also involved in the pathway. Therefore, retrovirus-mediated gene-trap mutagenesis (Ishida and Leder, 1999; Wiles et al., 2000; Guo et al., 2004) was used to isolate a mutant, which exhibits an increased tolerance to a simple alkylating agent that produces O^6-methylguanine. The disrupted gene in the mutant was identified to be a novel gene, designated Mapo1 (for O^6-methylguanine-induced apoptosis 1), which encodes a protein with a molecular mass of 125.6 kDa. Evidence is herein presented, which shows that the protein might be involved in the pathway of apoptosis induced by O^6-methylguanine adducts.

Results

Isolation of mutant cells defective in O^6-methylguanine-induced apoptosis

To perform insertional mutagenesis, we constructed a retrovirus-based gene-trap vector, pLHΔU3L, as illustrated in the upper part of Figure 1. The vector carries a promoterless hygromycin B resistance (Hyg^r) gene, together with a splice acceptor site and an internal ribosome entry site (IRES), which would facilitate efficient transcription and translation of the Hyg^r gene when integrated into any region, including an intron sequence, of actively transcribed genes. If the function of any gene indispensable for inducing apoptosis is lost by this insertional mutagenesis, we may expect that Mgmt-defective cells that are hypersensitive to a simple alkylating agent would become resistant to MNU. According to this experimental scheme (Figure 1), YT102 cells, a lung fibroblast cell line established from Mgmt-knockout mice (Takagi et al., 2003), were infected

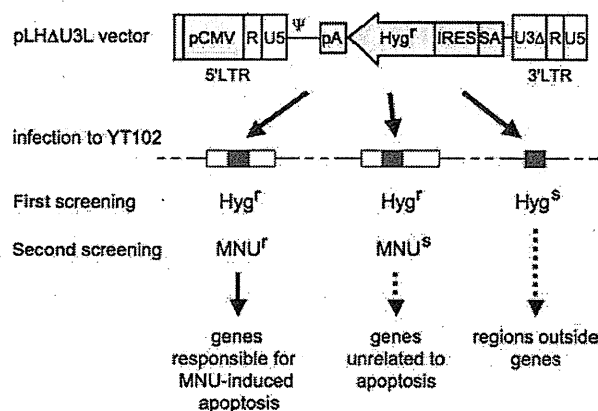Figure 1 Retrovirus-mediated gene-trap mutagenesis. Schematic diagram of the pLHΔU3L vector is drawn at the top. ψ, packaging signal; Hyg^R, hygromycin-resistant gene; IRES, internal ribosome entry site; LTR, long terminal repeat; pA, poly A signal; pCMV, cytomegalovirus promoter; SA, splicing acceptor site. Flowchart of the mutant screening is shown at the bottom. A line represents the genomic DNA. White boxes on the line indicate genes, into which vector DNA drawn as gray boxes is integrated. Hyg^r, hygromycin resistant; Hyg^s, hygromycin sensitive; MNU^r, MNU resistant; MNU^s, MNU sensitive.

with the gene-trap vector pLHΔU3L and hygromycin-resistant (Hyg^r) cells were obtained. The population of Hyg^r cells carrying the vector sequence within actively transcribed genes was then subjected to selection with 0.4 mM MNU. The MNU-resistant (MNU^r) clones were isolated as candidates that have insertional mutations within the genes involved in MNU-induced apoptosis.

O^6-Methylguanine, which is a major cytotoxic adduct produced in DNA by treating the cells with low doses of MNU, can be repaired by a specific DNA repair enzyme, MGMT. As shown in Figure 2, YT102 cells are defective in this enzyme and readily undergo cell death after exposure to relatively low doses of MNU. In contrast, YT102M, a derivative of YT102 that stably expresses human MGMT (Figure 2a), is resistant to the treatment with such doses of MNU, indicating that the cell death induced in YT102 cells results from O^6-methylguanine. One of the isolated mutants exhibited a significantly high level of resistance to MNU, in comparison to the parental cell line YT102, without expressing MGMT. The expression levels of MMR proteins, namely MSH2, MSH6, MLH1 and PMS2, which are required for the recognition of the O^6-methylguanine-mispaired lesions, were not affected in the mutant (Figure 2a). We termed this clone KH101 and performed a survival assay with various doses of MNU. As calculated from the survival curves shown in Figure 2b, the doses required to give LD_{37} to KH101 and the parental Mgmt$^{-/-}$ strain, YT102, are 0.48 and 0.08 mM, respectively. Therefore, KH101 is approximately six times more resistant to MNU than the parental Mgmt$^{-/-}$ strain, due to inactivation of a certain gene that might be required for apoptosis. The level of resistance of KH101, however, is lower in comparison to YT103, which lacks both MGMT and MLH1 functions.
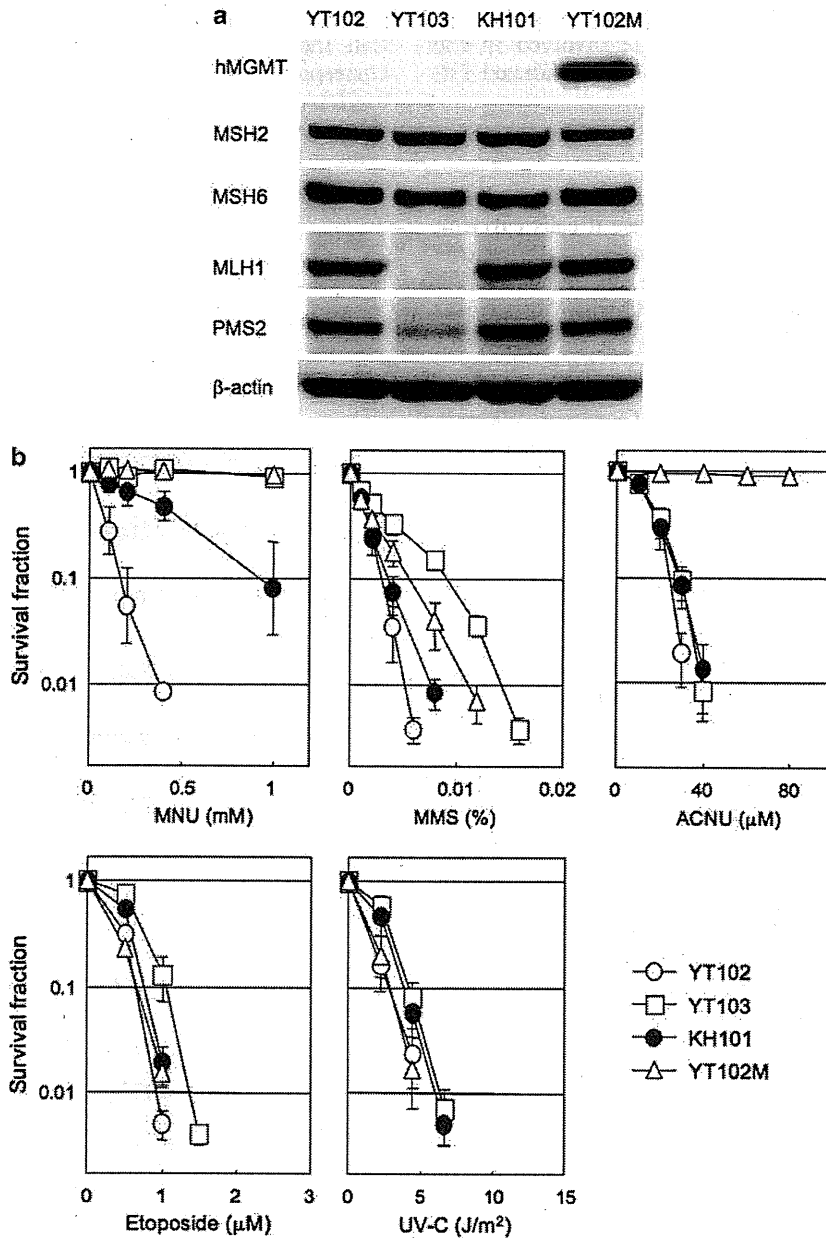
Figure 2 The sensitivities of various mutant cells to DNA-damaging agents. (a) The expression levels of O^6-methylguanine-DNA methyltransferase (MGMT) and mismatch repair (MMR) proteins in YT102, YT103, KH101 and YT102M cell lines. The MGMT and MMR proteins were detected with immunoblotting using specific antibodies. (b) The cells were treated with different concentrations of N-methyl-N-nitrosourea (MNU), methyl methanesulfonate (MMS) and 1-(4-amino-2-methyl-5-pyrimidinyl)methyl-3-(2-chloroethyl)-3-nitrosourea (ACNU) for 1 h, or etoposide for 12 h, and then were incubated in a drug-free medium for 6 days. For ultraviolet (UV) irradiation, the cells were exposed to different doses of UV-C. The numbers of colonies were counted and the survival fractions were determined. All experiments were performed three times and the standard deviations are shown in bars. Open circles, YT102 ($Mgmt^{-/-}$); open squares, YT103 ($Mgmt^{-/-}$ $Mlh1^{-/-}$); closed circles, KH101; open triangles, YT102M.

When treated with other DNA-damaging agents, methyl methanesulfonate (MMS), 1-(4-amino-2-methyl-5-pyri-midinyl)methyl-3-(2-chloroethyl)-3-nitrosourea (ACNU), etoposide and ultraviolet (UV)-C, which produce primarily N7-methylguanines and N3-methyladenines, DNA-interstrand crosslinks, DNA double-strand breaks and pyrimidine dimers, respectively, KH101 cells showed a similar degree of sensitivity to the parental strain YT102, although KH101 cells tended to be slightly more resistant than YT102 in all cases. YT103 and YT102M cells displayed increased resistance to MMS in comparison to YT102, as reported earlier (Kaina et al., 1991; Glaab et al., 1998). YT102 cells were quite resistant to ACNU as expected (Peng et al., 2007;

Sanada et al., 2007). These results imply that KH101 cells might have a defect in a gene involved in the induction of cell death caused by MNU-induced O^6-methylguanine.

MNU-induced mutant frequency

As O^6-methylguanine is a premutagenic DNA lesions, the mutation frequency would increase if cells carrying O^6-methylguanine are not eliminated by apoptosis (Takagi et al., 2003). Therefore, we measured the mutant frequency of KH101 cells with respect to ouabain resistance, which can arise by a mutation in the Na^+/K^+ ATPase locus (Figure 3). As a control, we used YT102M, which is resistant to MNU, for its overexpression of the human MGMT protein. Without MNU treatment, YT102M and KH101 cells exhibited the same low level of mutant frequency, indicating that the defect in KH101 cells does not affect the spontaneous mutagenesis. The mutant frequencies of both strains increased on exposure to MNU, but the extent of increase in KH101 was far greater than that of YT102M. The level attained with KH101 cells was about six times higher than that of YT102M. This is consistent with the possibility that the gene product defective in KH101 cells may be involved in a process to execute apoptosis in cells carrying mutation-evoking DNA lesions.

Identification of the gene defective in KH101 mutant

To determine the genomic sequence into which the vector DNA has been integrated, we carried out inverse PCR using the genomic DNAs digested with several restriction enzymes as templates. The amplified DNA fragments, spanning the junctions between the genomic DNA and the integrated vector sequences, were cloned into a pGEM-Teasy plasmid, and the nucleotide
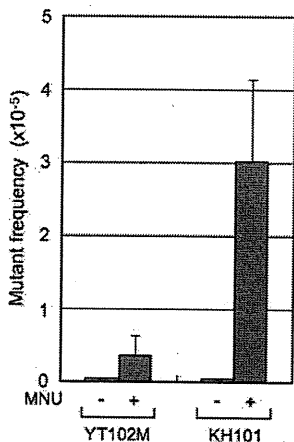
sequences were determined. A database search revealed that the vector DNA to be integrated in a sequence corresponding to the first intron of a putative gene mKIAA1450 (GenBank accession no. XM_907047) (Figure 4a), located in the E3 locus of mouse chromosome 3. The prospective gene is composed of at least 18 exons and would encode a polypeptide comprising 1138 amino acids. The gene is novel, and thus, we named it Mapo1. A homology search shows that the MAPO1-
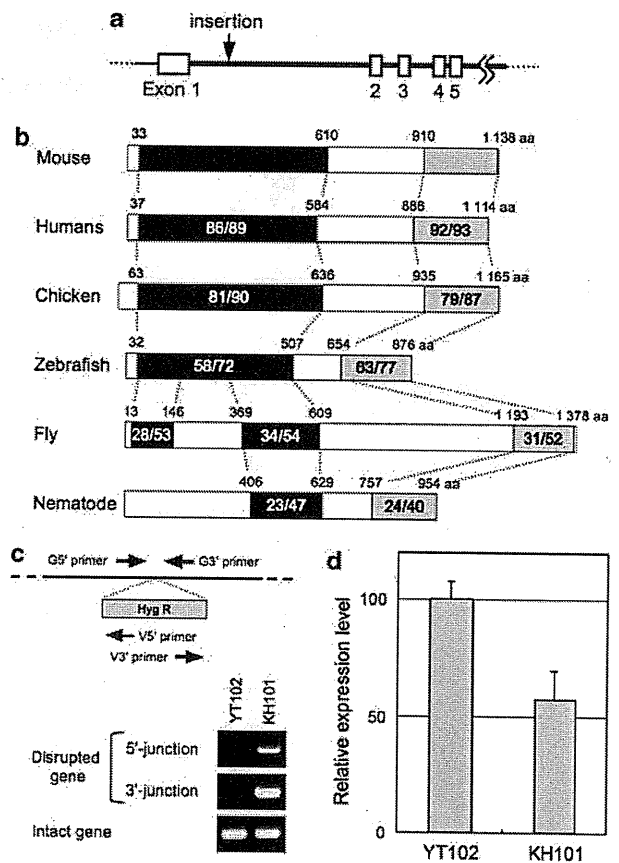

Figure 4 Structure and expression of the *Mapo1* gene. (a) A part of the gene in which the vector integration site is shown by an arrow. (b) Comparison of the MAPO1 proteins of various organisms. Accession numbers of the proteins are XP_912140 for mouse (*Mus musculus*), NP_065891 for humans (*Homo sapiens*), XP_420386 for chicken (*Gallus gallus*), XP_692808 for zebrafish (*Danio rerio*), NP_648943 for fly (*Drosophila melanogaster*) and NP_001023357 for nematode (*Caenorhabditis elegans*). The N- and C-terminal conserved regions, are shown by dark and light gray boxes, respectively. The numbers in the boxes indicate the percentages of amino acids showing identity/similarity in each conserved region of the proteins in comparison to those for mouse. The numbers above each box represent the amino-acid numbers beginning from the N-terminal ends of the proteins. (c) PCR analyses of the *Mapo1* gene in KH101 mutant cells. The upper panel shows the orientation and positions of four kinds of PCR primers designed for determination of the genomic and vector DNA sequences. The lower panel demonstrates the PCR-amplified 5'- and 3'-junctions of the wild-type and mutant forms of gene fragments. Amplified DNAs were separated by agarose gel electrophoresis and visualized by ethidium bromide staining. (d) The relative expression levels of the *Mapo1* gene as measured by quantitative real-time PCR.

Figure 3 Elevated mutant frequency after N-methyl-N-nitrosourea (MNU) treatment. YT102M, a derivative from YT102 that stably expresses the human O^6-methylguanine-DNA methyltransferase (MGMT) protein, and KH101 cells were treated with or without 0.4 mM MNU. After the treatment, the number of viable cells and ouabain-resistant cells were determined, and the mutant frequencies were calculated. The mean values obtained from three experiments and the standard deviations (bars) are presented.

1146

related sequences are present in a wide range of multicellular organisms ranging from humans to nematode, but not found in microorganisms, including budding and fission yeasts. There are highly conserved sequences in the amino- and the carboxyl-terminal regions of the protein (Figure 4b).

To determine whether either a single or both allele(s) of the gene was disrupted in the mutant, we performed PCR analyses using two sets of primers specific for the disrupted gene, G5′ + V5′ and V3′ + G3′ primers, and a G5′ + G3′ primer set for the intact sequence of wild-type allele (Figure 4c). In the sample from the KH101 mutant, signals for the 5′- and 3′-junctions of the Mapo1 gene and the vector DNA, and also a signal specific for the intact gene, were detected. In the sample derived from YT102, only a signal for the intact gene was found. These results suggest that one of the Mapo1 alleles was disrupted, whereas the other remains intact in KH101 cells. In proportion to the gene dosage, the expression level of the Mapo1 gene in KH101 ($Mapo1^{+/-}$) cells was approximately half the amount of that of YT102 ($Mapo1^{+/+}$) cells, as measured by quantitative real-time PCR (Figure 4d).

Suppression of the MAPO1 function by small interfering RNA

A synthetic small interfering RNA (siRNA) for the Mapo1 gene, siMapo1, was introduced into YT102 cells and its expression level was determined 48 h later. An siRNA composed of a sequence unrelated to the Mapo1 gene was also introduced as a control. The expression level of the Mapo1 gene in siMapo1-treated cells was reduced to 43% of that of cells that received the control RNA, siCont (Figure 5a). These two types of cells were treated with or without 1 mM MNU and, after incubation for 2, 3 and 4 days, were subjected to flow cytometric analysis to monitor the appearance of cells with a sub-G1 DNA content. After treatment with
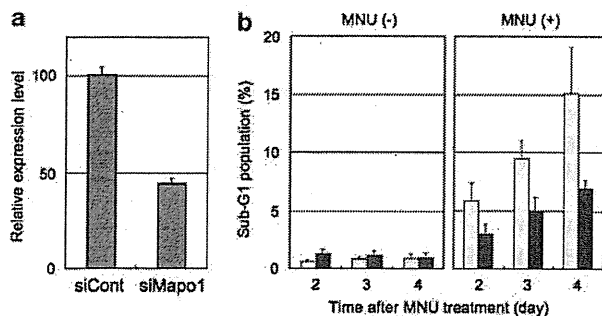
MNU, the sub-G1 cell population increased gradually in cells treated with either type of siRNA, but the degree of increase in cells treated with siRNA for Mapo1 was significantly lower than that obtained with control siRNA-treated cells (Figure 5b). A similar result was obtained by using siRNA that binds to a different region of Mapo1 sequence (data not shown). Therefore, a good correlation was observed between the Mapo1 expression level and the sub-G1 population in cell culture after MNU treatment. As an increase in the sub-G1 population represents the number of cells that undergo apoptotic cell death, these results suggest that the MAPO1 function is involved in O^6-methylguanine-induced apoptosis.

Effects of Mapo1 mutation on apoptosis-related events

We analysed the levels of the phosphorylation of p53, CHK1 and histone H2AX (γH2AX), which are believed to be the downstream targets of ATR kinase, when the cells were treated with MNU (Cejka et al., 2003; Stojic et al., 2004). As shown in Figure 6a, the MNU-induced phosphorylation of these proteins was clearly observed,
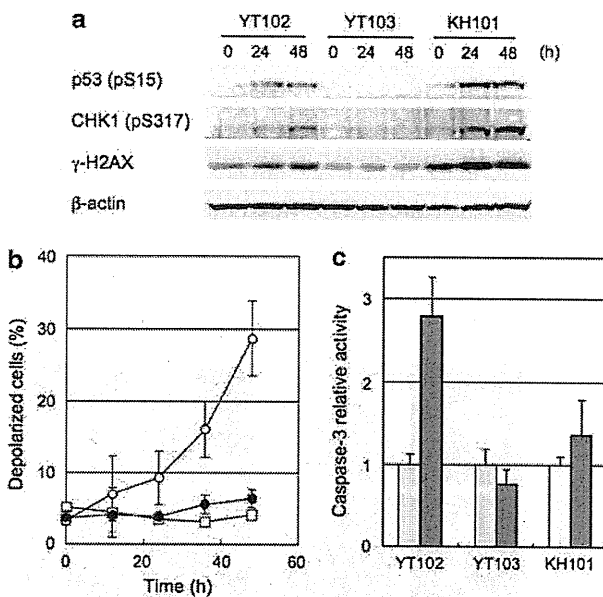

Figure 6 The expression of apoptosis-related activities in KH101 cells. (a) The activation of DNA damage signaling after exposure to N-methyl-N-nitrosourea (MNU). The phosphorylation of p53, CHK1 and histone H2AX was monitored by immunoblotting. β-Actin is a loading control. (b) Mitochondrial membrane depolarization after treatment with MNU. Cells were treated with 0.48 mM MNU for 1 h and further incubated. At the times indicated, cells were collected and applied to a mitochondrial membrane depolarization assay. The numbers of depolarized cells were counted by using a flow cytometer and the ratios were plotted. Open circles, YT102; open squares, YT103; closed circles, KH101. (c) Induction of caspase-3 activity after MNU treatment. Caspase-3 activity was determined at 72 h after treatment with or without 0.4 mM MNU. The values obtained with the MNU-treated cells were divided by those for the untreated cells, and the relative caspase-3 activities are shown. Light and dark columns represent the values for cells treated without and with MNU, respectively. All experiments were performed three times and the standard deviations are shown in bars.

Figure 5 Suppression of apoptosis by small interfering RNA (siRNA) for Mapo1. (a) The expression levels of the Mapo1 gene in YT102 ($Mgmt^{-/-}$) cells treated with control and Mapo1 siRNA, as measured by real-time PCR. (b) Sub-G1 population in YT102 cells treated with control and Mapo1 siRNA after N-methyl-N-nitrosourea (MNU) application. At 2 days after the application of either type of siRNA, YT102 cells were treated with or without 1 mM MNU for 1 h and then incubated for several days. At various times after MNU treatment, cells were harvested and subjected to a flow cytometric analysis. Light and dark columns represent sub-G1 population (%) for control siRNA- and Mapo1 siRNA-treated cells, respectively.

after treatment with MNU, in KH101 as well as YT102 cells, although such phosphorylation was not shown in *Mlh1*-deficient YT103. These results indicate that the *Mapo1* mutation does not impair the MMR-dependent DNA damage detection and signaling.

We further examined the effect of *Mapo1* mutation on the depolarization of the mitochondrial membrane, which is known to occur during the process of apoptosis (Cossarizza et al., 1994). As expected, the depolarization of mitochondria is induced gradually in YT102 (*Mgmt*$^{-/-}$) cells after treatment with MNU (Figure 6b). However, no such depolarization was observed with KH101 (*Mgmt*$^{-/-}$ *Mapo1*$^{+/-}$) cells or with YT103 (*Mgmt*$^{-/-}$ *Mlh1*$^{-/-}$). To obtain further evidence that KH101 mutant cells are defective in a certain step in the process of apoptosis, we measured caspase-3 activity. Figure 6c shows levels of caspase-3 activity after treatment of the three types of cells with 0.4 mM MNU. Caspase-3 activity of YT102 cells increased three times the level of the untreated cells, whereas no increase was observed with YT103 cells. In KH101 cells, the level of caspase-3 activity after MNU treatment was as low as that of the untreated control. These results further support the notion that KH101 cells might have a defect in a certain step of the O^6-methylguanine-induced apoptosis pathway.

Cytoplasmic localization of EGFP-fused MAPO1 proteins
To analyse the subcellular localization of the MAPO1 protein, we have cloned the full-length mouse *Mapo1* cDNA and expressed EGFP-fused mMAPO1 protein in

Figure 7 Cytoplasmic localization of MAPO1 proteins. The plasmid DNAs expressing EGFP-fused mouse and human MAPO1 proteins were transfected into YT102 and HeLa MR, respectively. After 24 h, the cells were treated with or without 0.4 mM *N*-methyl-*N*-nitrosourea (MNU) for 1 h. After another 24 h incubation, the cells were washed with phosphate-buffered saline (PBS) and stained with 10 μM of Hoechst33342 followed by the analyses using fluorescent microscopy. The images for EGFP-fused MAPO1, Hoechst33342 signals and phase contrast are represented at the top, middle and bottom, respectively. (a) Images of cells expressing EGFP-fused mMAPO1. (b) Images of cells expressing EGFP-fused hMAPO1.

YT102 cells. As shown in Figure 7a, transiently expressed mMAPO1 protein is predominantly present in the cytoplasm. The cytoplasmic localization of mMAPO1 protein did not dramatically change even after treatment of cells with MNU. To assess whether this is the case for the highly conserved human ortholog, we also obtained the human cDNA for the gene and expressed EGFP-fused hMAPO1 protein in HeLa MR cells (Figure 7b). Similarly, the cytoplasmic localization of hMAPO1 was observed and it was found to be unaffected by the MNU treatment.

Discussion

There are two distinct types of DNA lesions that induce apoptosis: modified bases that cause base mispairing and bulky DNA lesions that block DNA replication. The former requires MMR proteins for induction of apoptosis, whereas the latter induces apoptosis even without the function of such proteins. O^6-Methylguanine, produced in DNA by the action of simple alkylating agents, does not prevent the progression of DNA replication forks and apparently represents the former class DNA lesion (Singer et al., 1989; Haracska et al., 2000). During DNA replication, O^6-methylguanine (O^6-meG) can pair with thymine as well as cytosine, and unless repaired, the resulting O^6-meG:T mispair would lead to mutations after next round of replication. To suppress such an outcome, organisms have been equipped with a mechanism for eliminating cells carrying mutation-evoking DNA lesions. The MMR protein complex apparently acts as a molecular device to detect such lesions. The MutSα, consisting of MSH2 and MSH6, and PCNA complex first recognizes O^6-meG:T mispair in DNA and then MutLα, composed of MLH1 and PMS2, binds to the initial complex. The formation of the mismatch recognition complex is indispensable for the activation of DNA damage signaling as well as the induction of apoptosis (Hidaka et al., 2005; Yoshioka et al., 2006; Sanada et al., 2007).

The precise molecular mechanism of signal transduction downstream of mismatch recognition still remains to be determined. As many proteins would be involved in this process, we have initiated the present study to identify such proteins by gene-trap mutagenesis screening. As a selectable marker for the gene trap, a promoterless hygromycin B resistance gene placed near a splicing acceptor and an IRES sequences was used. This allowed efficient expression of the marker, when it was integrated into any region of actively transcribed genes to be mutated. Among Hyg^r cells selected, candidate clones could be obtained that might have defects in an apoptosis-related process. In this way, we were able to identify *Mapo1*, which turned out to be a novel gene involved in O^6-methylguanine-induced apoptosis. The *Mapo1* encodes a protein with a molecular mass of 125.6 kDa, carrying no characteristic functional motifs. The MAPO1 sequence, however, has the highly conserved amino- and carboxyl-terminal domains present in various multicellular organisms
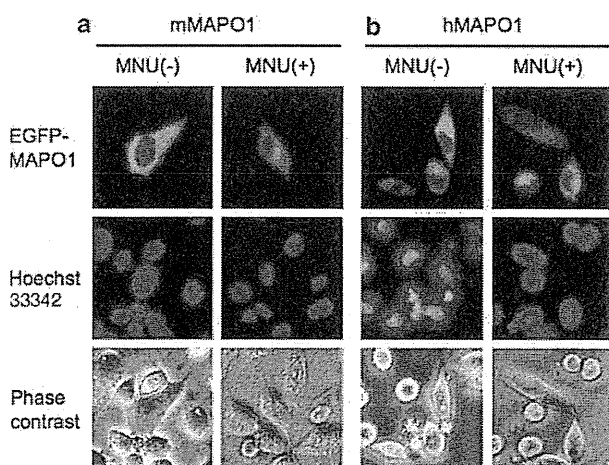
ranging from humans to nematode, but not in micro-organisms including yeast. This evolutional conservation might reflect its possible biological significance on the apoptosis in multicellular organisms.

In the present study, we show that $Mapo1$ mutation renders the cells significantly resistant to MNU, although it does not dramatically affect its sensitivity to the killing effect caused by MMS, ACNU, etoposide or UV irradiation (Figure 2). Importantly, even when the $Mapo1$-defective KH101 cells are treated with MNU, the depolarization of the mitochondrial membrane and caspase-3 activation, hallmarks of apoptosis induction, are significantly suppressed. As the phosphorylation of p53, CHK1 and histone H2AX, downstream targets of ATR kinase, is nevertheless observed in KH101 cells after MNU treatment (Figure 6), the MAPO1 protein, which is localized in the cytoplasm (Figure 7), is not likely to be involved in the nuclear translocation of MutSα complex (Christmann and Kaina, 2000) nor in the activation of MNU-induced DNA damage signaling. These results suggest that MAPO1 may play a role in a certain step(s) of the signal-transduction pathway of apoptosis, induced by the O⁶-methylguanine, that would activate the apoptotic function of the mitochondria.

It is remarkable that the $Mapo1$ mutation exerts its effect even when one of the alleles is intact. KH101 ($Mgmt^{-/-}Mapo1^{+/-}$) cells exhibit a significantly higher level of resistance to MNU than YT102 ($Mgmt^{-/-}$ $Mapo1^{+/+}$) cells. We have also shown that MNU-induced apoptosis, as measured by an increase in the sub-G1 population, is significantly suppressed when the expression level of $Mapo1$ is reduced to half its normal level by siRNA treatment. This haploinsufficient character of the $Mapo1$ gene is reminiscent of the phenomenon observed with MMR-related genes. $Mgmt^{-/-}$ $Mlh1^{+/-}$ cells, which carry almost half the amount of MLH1 protein in comparison with $Mlh1^{+/+}$ cells, are substantially resistant to the killing action of MNU than are $Mgmt^{-/-}Mlh1^{+/+}$ cells (Kawate et al., 2000; Cejka et al., 2003; Takagi et al., 2003). This haploinsufficient nature may be related to the fact that MLH1 protein forms a heterodimer with PMS2 to form a MutLα complex (Li and Modrich, 1995). MutLα further binds to MutSα, which is composed of MSH2 and MSH6, and participates in the recognition of mismatch bases in DNA to initiate the apoptotic reaction. Thus, these mismatch recognition proteins act in a stoichiometric manner, rather than in a catalytic one, in inducing the apoptotic signal. As the $Mapo1$ exhibits a similar phenotype, it may exert its function by forming a complex with other components, rather than by acting in a catalytic manner or by changing the localization of the protein.

To obtain further insight into the $Mapo1$ function, it is necessary to establish a cell line defective in both of the alleles of the gene. The neomycin selection method, which is usually used to isolate such clones, cannot be applied to the present study, as the neomycin-resistant marker was already introduced into the parental strain to knockout the $Mgmt$ gene. Other strategies are now being applied to isolate such doubly deficient cells that might show a higher level of resistance to the MNU treatment.

Materials and methods

Cell lines and cell culture
YT102 ($Mgmt^{-/-}Mlh1^{+/+}$) and YT103 ($Mgmt^{-/-}Mlh1^{-/-}$) are cell lines established, by expressing SV40 T antigen, from primary cells consisting of fibroblasts derived from the lung tissue of $Mgmt$ and $Mgmt$ $Mlh1$-knockout mice, respectively (Takagi et al., 2003). YT102M is a derivative of YT102 that carries the expression vector, pIREShyg2:$Mgmt$ (Takagi et al., 2003), to stably express human MGMT. The cells were cultivated in Dulbecco's modified Eagle's medium supplemented with 10% fetal bovine serum (FBS) at 37 °C in 5% CO_2.

Gene-trap mutagenesis and screening for MNUʳ clones
The retrovirus vector, pLHΔU3L, which carries the hygromycin B resistance gene, was constructed for the gene-trap mutagenesis. The promoter region in 3′LTR of a retroviral vector, pDON-AI (Takara Bio Inc., Ohtsu, Japan), was removed by AflII and XbaI digestion followed by self-ligation. The SV40 promoter and the neomycin resistance gene were removed from the vector by digestion with SalI and XhoI, and then the loxP²-containing fragment, which was excised from the pBS246 vector (Invitrogen, Carlsbad, CA, USA) by NotI digestion, was inserted into the site after blunt ending. A DNA fragment containing synthetic intron (IVS), IRES, hygromycin B resistance gene and poly A signal sequences was isolated from pIREShyg2 vector (Clontech, Mountain View, CA, USA), and then inserted into the EcoRV site in the loxP² region of the retroviral vector. The resulting pLHΔU3L vector was introduced into ΨMP34 (Takara Bio Inc.) cells by using Lipofectamine 2000 (Invitrogen) according to the manufacturer's instructions. After incubation of the cells for 1.5 days at 33 °C, the retroviral particles carrying the gene-trap construct in the medium were recovered and filtered.

Approximately 1.5×10^7 of YT102 cells grown on twenty 10-cm dishes were infected with the retrovirus and incubated for 15 h. The cells were further cultivated in a virus-free fresh medium for another day and then selected in a medium containing 0.6 mg/ml of hygromycin B for 55 h. After washing with phosphate-buffered saline (PBS) three times, the cells were treated with 0.4 mM MNU in serum-free medium for 1 h and further incubated in complete medium containing 10% FBS. Colonies formed were subjected to a quantitative cell survival assay with various concentrations of MNU. Finally, MNUʳ mutant cell lines were thus obtained.

Immunoblotting
Whole cell extracts were prepared by the lyses of cells with 2 × SDS–polyacrylamide gel electrophoresis (PAGE) sample buffer (120 mM Tris–HCl (pH 6.8), 4% SDS, 20% glycerol, 200 mM dithiothreitol and 0.002% bromophenol blue) and then subjected to SDS–PAGE and electroblotted onto a PVDF membrane (Bio-Rad, Hercules, CA, USA). Detection was performed using an ECL Plus or Advance western blotting detection kit (GE Healthcare, Buckinghamshire, UK). The primary antibodies used were: anti-MGMT (BD Pharmingen, San Diego, CA, USA), anti-MSH2 (Zymed, San Francisco, CA, USA), anti-MSH6 (BD Transduction, San Jose, CA, USA), anti-MLH1 (Santa Cruz, Santa Cruz, CA, USA), anti-PMS2 (BD Pharmingen), anti-β-actin (Sigma, St Louis, MO, USA), anti-phospho-p53 (Ser15) (Cell Signaling, Danvers, MA, USA), anti-phospho-CHK1 (Ser317) (Bethyl, Montgomery, TX, USA) and anti-phospho-histone H2AX (Ser139) (Upstate, Temecula, CA, USA).

Survival of cells treated with MNU, MMS, ACNU etoposide and UV-C
The cells were treated with various concentrations of MNU, MMS or ACNU in serum-free medium for 1 h, etoposide in a medium containing 10% FBS for 12 h, or irradiated with different doses of UV-C. After cultivation with a medium containing 10% FBS for 6 days, the number of colonies was counted and the survival rate was calculated.

Measurement of mutant frequency
The cells were treated with 0 or 0.4 mM MNU as described above and incubated for 4 days. Then, the cells were placed in a medium containing 2 mM ouabain for 10 days. After staining, the number of resistant colonies was counted. In parallel, a cell suspension containing about 500 cells was seeded in several dishes and the number of viable cells was counted.

Analyses of the disrupted gene by PCR
For inverse PCR, 10 μg of genomic DNA prepared from KH101 mutant cells was digested with *Bam*HI and *Bgl*II, or *Hind*II restriction enzymes. Precipitated DNA was resuspended in 1 ml of buffer (66 mM Tris–HCl; pH 7.6, 6.6 mM MgCl₂, 10 mM dithiothreitol and 0.1 mM ATP) and incubated at 16 °C overnight after adding 1750 U of T4 DNA ligase (Takara Bio Inc.). By using the DNA as a template, 5′- and 3′-junctions between the disrupted gene and the vector DNA were amplified by PCR with two primer sets designed for the vector sequence, GS1: 5′-AGCTTACCTCCCGGTGGTGGG TCGGTGGTC-3′ and DON1: 5′-GCGGGGGCGACTTCG GCTCACAGCGCGCCC-3′ or US1: 5′-CTTGTGGTCTCG CTGTTCCTTGGGAGGGTC–3′ and UR1: 5′-GGGGCACC CTGGAAACATCTGATGGTTCTC-3′, respectively. The DNA fragments amplified were cloned into a pGEM-Teasy vector (Promega, Madison, WI, USA). The nucleotide sequences of the clones were determined and analysed in NCBI GenBank.

For the detection of the mutant allele, DNA fragments specific for the disrupted *Mapo1* gene or for the intact gene were amplified by PCR, using primer sets, G5′ + V5′ and V3′ + G3′, or G5′ + G3′, respectively. The nucleotide sequences of PCR primers are G5′, 5′-ATGCTAAAGTAGCTT GTTGTGGGCCTTTCC-3′; G3′, 5′-CGCTCATACAAGCA GTTAGCAACCGC-3′; V5′, 5′-ATTTAGTCTCCAGAAAA AGGGGGGAATG-3′ and V3′, 5′-AGCTTACCTCCCGGT GGTGGGTCGGTGGTC-3′.

Measurement of gene expression by real-time PCR
Total RNA was prepared from cells grown on a six-well plate using the RNeasy Mini kit (Qiagen, Hilden, Germany) and were used to synthesize cDNAs by using PrimeScript Reverse Transcriptase (Takara Bio Inc.). Real-time PCR was performed with a light cycler (Roche, Mannheim, Germany) using SYBR Premix Ex Taq (Takara Bio Inc.). The PCR primers for a *Mapo1* gene, pMapo1-F and pMapo1-R, and for a *Gapdh* gene as a reference, pmGapdh-F and pmGapdh-R, were purchased from Takara Bio Inc. and the nucleotide sequences are pMapo1-F, 5′-GCACACAGCACACCTGTTGA-3′; pMapo1-R, 5′-GCGCTGGTAACTGCTGGAA-3′; pmGapdh-F, 5′-AAATGGTGAAGGTCGGTGTG-3′; pmGapdh-R, 5′-TGA AGGGGTCGTTGATGG-3′.

siRNA transfection
Stealth RNAi for the *Mapo1* sequence (siMapo1), 5′-CA GAAAGCAGAGGATGTTCCTATTA-3′, was purchased from Invitrogen. After culturing 1 × 10⁵ cells in a six-well plate for 1 day, the cells were transfected with 20 nM siRNA, using the Lipofectamine RNAiMAX reagent (Invitrogen) according to the manufacturer's protocol. For the control transfection, Stealth RNAi Negative Control Medium GC Duplex (Invitrogen) was used.

Mitochondrial membrane depolarization assay
About 2 × 10⁵ cells were washed with PBS and treated with 0.48 mM MNU for 1 h. The doses of the drugs correspond to six lethal hits for YT102 cells, as calculated from the survival curves. The cells were further incubated in complete medium and collected at 0, 12, 24, 36 and 48 h after the treatment with MNU. The mitochondrial membrane potential assay was performed using the MitoProbe DiOC2(3) Assay kit (Invitrogen), as described earlier (Takagi et al., 2008).

Molecular cloning of Mapo1 *cDNAs*
To clone mouse *Mapo1* cDNA, RT–PCR reactions were carried out to amplify four parts of cDNA with overlapping sequences using cDNAs, synthesized from total RNA prepared from YT102 cells, as templates. The four cDNA fragments were connected to each other at the internal restriction sites and the full-length mouse *Mapo1* cDNA was thus generated. The human *Mapo1* cDNA (KIAA1450) was obtained from the Kazusa DNA Research Institute (Kisarazu, Japan).

Expression of EGFP-fused MAPO1 protein and microscopic analysis
To construct plasmids to express MAPO1 proteins fused with EGFP at the C-terminal regions, we introduced mouse and human *Mapo1* cDNA together with the EGFP gene into *Eco*RV and *Not*I site of pIRESpuro2 (Clontech) plasmid. To express the EGFP-fused MAPO1 proteins, 0.8 μg of plasmid DNAs was transfected using Lipofectamine 2000 into YT102 (for mouse) or HeLa MR (for humans) cells growing in 24-well plates according to the manufacturer's instructions. The cells were treated with or without 0.4 mM MNU for 1 h at 24 h after transfection. After another 24-h incubation, the cells were washed with PBS and stained with 10 μM of Hoechst33342 (Invitrogen) and fluorescent signals were observed by fluorescent microscopy (Nikon, Tokyo, Japan).

Other methods
Flow cytometric analysis and of caspase-3 activity assay were performed as described earlier (Hidaka et al., 2005).

Acknowledgements

Conflict of interest

The authors declare no conflict of interest.

References

Beranek DT. (1990). Distribution of methyl and ethyl adducts following alkylation with monofunctional alkylating agents. *Mutat Res* **231**: 11–30.

Branch P, Aquilina G, Bignami M, Karran P. (1993). Defective mismatch binding and a mutator phenotype in cells tolerant to DNA damage. *Nature* **362**: 652–654.

Caporali S, Falcinelli S, Starace G, Russo MT, Bonmassar E, Jiricny J et al. (2004). DNA damage induced by temozolomide signals to both ATM and ATR: role of the mismatch repair system. Mol Pharmacol 66: 478–491.

Cejka P, Stojic L, Mojas N, Russell AM, Heinimann K, Cannavo E et al. (2003). Methylation-induced G(2)/M arrest requires a full complement of the mismatch repair protein hMLH1. EMBO J 22: 2245–2254.

Christmann M, Kaina B. (2000). Nuclear translocation of mismatch repair proteins MSH2 and MSH6 as a response of cells to alkylating agents. J Biol Chem 275: 36256–36262.

Cossarizza A, Kalashnikova G, Grassilli E, Chiappelli F, Salvioli S, Capri M et al. (1994). Mitochondrial modifications during rat thymocyte apoptosis: a study at the single cell level. Exp Cell Res 214: 323–330.

Coulondre C, Miller JH. (1977). Genetic studies of the lac repressor. IV. Mutagenic specificity in the lacI gene of Escherichia coli. J Mol Biol 117: 577–606.

Fishel R. (1998). Mismatch repair, molecular switches, and signal transduction. Genes Dev 12: 2096–2101.

Glaab WE, Risinger JI, Umar A, Barrett JC, Kunkel TA, Tindall KR. (1998). Cellular resistance and hypermutability in mismatch repair-deficient human cancer cell lines following treatment with methyl methanesulfonate. Mutat Res 398: 197–207.

Glassner BJ, Weeda G, Allan JM, Broekhof JL, Carls NH, Donker I et al. (1999). DNA repair methyltransferase (Mgmt) knockout mice are sensitive to the lethal effects of chemotherapeutic alkylating agents. Mutagenesis 14: 339–347.

Guo G, Wang W, Bradley A. (2004). Mismatch repair genes identified using genetic screens in Blm-deficient embryonic stem cells. Nature 429: 891–985.

Haracska L, Prakash S, Prakash L. (2000). Replication past O⁶-methylguanine by yeast and human DNA polymerase eta. Mol Cell Biol 20: 8001–8007.

Hickman MJ, Samson LD. (1999). Role of DNA mismatch repair and p53 in signaling induction of apoptosis by alkylating agents. Proc Natl Acad Sci USA 96: 10764–10769.

Hickman MJ, Samson LD. (2004). Apoptotic signaling in response to a single type of DNA lesion, O⁶-methylguanine. Mol Cell 14: 105–116.

Hidaka M, Takagi Y, Takano TY, Sekiguchi M. (2005). PCNA-MutSalpha-mediated binding of MutLalpha to replicative DNA with mismatched bases to induce apoptosis in human cells. Nucleic Acids Res 33: 5703–5712.

Ishida Y, Leder P. (1999). RET: a poly A-trap retrovirus vector for reversible disruption and expression monitoring of genes in living cells. Nucleic Acids Res 27: e35.

Ito T, Nakamura T, Maki H, Sekiguchi M. (1994). Roles of transcription and repair in alkylation mutagenesis. Mutat Res 314: 273–285.

Kaina B, Christmann M, Naumann S, Roos WP. (2007). MGMT: key node in the battle against genotoxicity, carcinogenicity and apoptosis induced by alkylating agents. DNA Repair (Amst) 6: 1079–1099.

Kaina B, Fritz G, Mitra S, Coquerelle T. (1991). Transfection and expression of human O⁶-methylguanine-DNA methyltransferase (MGMT) cDNA in Chinese hamster cells: the role of MGMT in protection against the genotoxic effects of alkylating agents. Carcinogenesis 12: 1857–1867.

Karran P. (2001). Mechanisms of tolerance to DNA damaging therapeutic drugs. Carcinogenesis 22: 1931–1937.

Kat A, Thilly WG, Fang WH, Longley MJ, Li GM, Modrich P. (1993). An alkylation-tolerant, mutator human cell line is deficient in strand-specific mismatch repair. Proc Natl Acad Sci USA 90: 6424–6428.

Kawate H, Itoh R, Sakumi K, Nakabeppu Y, Tsuzuki T, Ide F et al. (2000). A defect in a single allele of the Mlh1 gene causes dissociation of the killing and tumorigenic actions of an alkylating

carcinogen in methyltransferase-deficient mice. Carcinogenesis 21: 301–305.

Kawate H, Sakumi K, Tsuzuki T, Nakatsuru Y, Ishikawa T, Takahashi S et al. (1998). Separation of killing and tumorigenic effects of an alkylating agent in mice defective in two of the DNA repair genes. Proc Natl Acad Sci USA 95: 5116–5120.

Li G, Modrich P. (1995). Restoration of mismatch repair to nuclear extracts of H6 colorectal tumor cells by a heterodimer of human MutL homologs. Proc Natl Acad Sci USA 92: 1950–1954.

Loechler EL, Green CL, Essigmann JM. (1984). In vivo mutagenesis by O⁶-methylguanine built into a unique site in a viral genome. Proc Natl Acad Sci USA 81: 6271–6275.

Margison GP, Santibanez-Koref MF. (2002). O⁶-alkylguanine-DNA alkyltransferase: role in carcinogenesis and chemotherapy. Bioessays 24: 255–266.

Meikrantz W, Bergom MA, Memisoglu A, Samson L. (1998). O⁶-alkylguanine DNA lesions trigger apoptosis. Carcinogenesis 19: 369–372.

Ochs K, Kaina B. (2000). Apoptosis induced by DNA damage O⁶-methylguanine is Bcl-2 and caspase-9/3 regulated and Fas/caspase-8 independent. Cancer Res 60: 5815–5824.

Pegg AE. (2000). Repair of O(6)-alkylguanine by alkyltransferases. Mutat Res 462: 83–100.

Peng M, Litman R, Xie J, Sharma S, Brosh Jr RM, Cantor SB. (2007). The FANCJ/MutLalpha interaction is required for correction of the cross-link response in FA-J cells. EMBO J 26: 3238–3249.

Pepponi R, Marra G, Fuggetta MP, Falcinelli S, Pagani E, Bonmassar E et al. (2003). The effect of O⁶-alkylguanine-DNA alkyltransferase and mismatch repair activities on the sensitivity of human melanoma cells to temozolomide, 1,3-bis(2-chloroethyl)1-nitrosourea, and cisplatin. J Pharmacol Exp Ther 304: 661–668.

Sakumi K, Shiraishi A, Shimizu S, Tsuzuki T, Ishikawa T, Sekiguchi M. (1997). Methylnitrosourea-induced tumorigenesis in MGMT gene knockout mice. Cancer Res 57: 2415–2418.

Sanada M, Hidaka M, Takagi Y, Takano TY, Nakatsu Y, Tsuzuki T et al. (2007). Modes of actions of two types of anti-neoplastic drugs, dacarbazine and ACNU, to induce apoptosis. Carcinogenesis 28: 2657–2663.

Singer B, Chavez F, Goodman MF, Essigmann JM, Dosanjh MK. (1989). Effect of 3′ flanking neighbors on kinetics of pairing of dCTP or dTTP opposite O⁶-methylguanine in a defined primed oligonucleotide when Escherichia coli DNA polymerase I is used. Proc Natl Acad Sci USA 86: 8271–8274.

Stojic L, Mojas N, Cejka P, Di Pietro M, Ferrari S, Marra G et al. (2004). Mismatch repair-dependent G2 checkpoint induced by low doses of SN1 type methylating agents requires the ATR kinase. Genes Dev 18: 1331–1344.

Takagi Y, Hidaka M, Sanada M, Yoshida H, Sekiguchi M. (2008). Different initial steps of apoptosis induced by two types of antineoplastic drugs. Biochem Pharmacol 76: 303–311.

Takagi Y, Takahashi M, Sanada M, Ito R, Yamaizumi M, Sekiguchi M. (2003). Roles of MGMT and MLH1 proteins in alkylation-induced apoptosis and mutagenesis. DNA Repair (Amst) 2: 1135–1146.

Tominaga Y, Tsuzuki T, Shiraishi A, Kawate H, Sekiguchi M. (1997). Alkylation-induced apoptosis of embryonic stem cells in which the gene for DNA-repair, methyltransferase, had been disrupted by gene targeting. Carcinogenesis 18: 889–896.

Tsuzuki T, Sakumi K, Shiraishi A, Kawate H, Igarashi H, Iwakuma T et al. (1996). Targeted disruption of the DNA repair methyltransferase gene renders mice hypersensitive to alkylating agent. Carcinogenesis 17: 1215–1220.

Wiles MV, Vauti F, Otte J, Fuchtbauer EM, Ruiz P, Fuchtbauer A et al. (2000). Establishment of a gene-trap sequence tag library to generate mutant mice from embryonic stem cells. Nat Genet 24: 13–14.

Yoshioka K, Yoshioka Y, Hsieh P. (2006). ATR kinase activation mediated by MutSalpha and MutLalpha in response to cytotoxic O⁶-methylguanine adducts. Mol Cell 22: 501–510.

DinB Upregulation Is the Sole Role of the SOS Response in Stress-Induced Mutagenesis in *Escherichia coli*

Rodrigo S. Galhardo,* Robert Do,* Masami Yamada,[†] Errol C. Friedberg,[‡] P. J. Hastings,*
Takehiko Nohmi[‡] and Susan M. Rosenberg*[,§,1]

*Department of Molecular and Human Genetics, Baylor College of Medicine, Houston, Texas 77030-3411, [‡]Department of Pathology, University of Texas Southwestern Medical Center, Dallas, Texas 5390-9072, [†]Division of Genetics and Mutagenesis, National Institute of Health Sciences, Tokyo 158-8501, Japan and [§]Departments of Biochemistry and Molecular Biology and Molecular Virology and Microbiology, The Dan L. Duncan Cancer Center, Baylor College of Medicine, Houston, Texas 77030-3411

ABSTRACT

Stress-induced mutagenesis is a collection of mechanisms observed in bacterial, yeast, and human cells in which adverse conditions provoke mutagenesis, often under the control of stress responses. Control of mutagenesis by stress responses may accelerate evolution specifically when cells are maladapted to their environments, *i.e.*, are stressed. It is therefore important to understand how stress responses increase mutagenesis. In the *Escherichia coli* Lac assay, stress-induced point mutagenesis requires induction of at least two stress responses: the RpoS-controlled general/starvation stress response and the SOS DNA-damage response, both of which upregulate DinB error-prone DNA polymerase, among other genes required for Lac mutagenesis. We show that upregulation of DinB is the only aspect of the SOS response needed for stress-induced mutagenesis. We constructed two *dinB*(o^c) (operator-constitutive) mutants. Both produce SOS-induced levels of DinB constitutively. We find that both *dinB*(o^c) alleles fully suppress the phenotype of constitutively SOS-"off" *lexA*(Ind$^-$) mutant cells, restoring normal levels of stress-induced mutagenesis. Thus, *dinB* is the only SOS gene required at induced levels for stress-induced point mutagenesis. Furthermore, although spontaneous SOS induction has been observed to occur in only a small fraction of cells, upregulation of *dinB* by the *dinB*(o^c) alleles in all cells does not promote a further increase in mutagenesis, implying that SOS induction of DinB, although necessary, is insufficient to differentiate cells into a hypermutable condition.

GENOMIC stability and mutation rates are tightly regulated features of all organisms. Understanding how cells regulate mutation rates has important implications for evolution, cancer progression and chemotherapy resistance, aging, and acquisition of antibiotic resistance and evasion of the immune system by pathogens, all processes driven by mutagenesis and all of which occur during stress.

Stress-induced mutagenesis refers to a group of related phenomena in which cells poorly adapted to their environment (*i.e.*, stressed) increase mutation rates as part of a regulated stress response (reviewed by GALHARDO *et al.* 2007). Abundant examples, particularly in microorganisms, show the induction of specific pathways of mutagenesis in response to stresses. The types of genetic alteration induced by stress include base substitutions, small deletions and insertions, gross chromo-

somal rearrangements and copy-number variations, and movement of mobile elements. These various pathways require the functions of different sets of genes and proteins. Thus, there appear to be multiple molecular mechanisms of stress-inducible mutagenesis that operate in different organisms, cell types, and growth-inhibiting stress conditions.

However, a common theme in the many mechanisms of stress-inducible mutagenesis described to date is the requirement for the function of one or more cellular stress responses. Starvation stress-induced mutagenesis in *Bacillus subtilis* requires the *comK* regulatory gene that controls the stress response that in turn allows competence for natural transformation in response to starvation (SUNG and YASBIN 2002). The RpoS-controlled general or starvation stress response is required for starvation-induced excisions of phage Mu in *Escherichia coli* (GOMEZ-GOMEZ *et al.* 1997), for base-substitution mutagenesis in aging *E. coli* colonies (BJEDOV *et al.* 2003), for starvation-induced point mutations (SAUMAA *et al.* 2002) and transpositions (ILVES *et al.* 2001) in *Pseudomonas putida*, and for starvation-induced gene amplification (LOMBARDO *et al.* 2004) and frameshift

mutagenesis (LAYTON and FOSTER 2003; LOMBARDO *et al.* 2004) in the *E. coli* Lac assay, described in more detail below. The SOS DNA-damage stress response is required for the stress-induced frameshift mutagenesis in the *E. coli* Lac assay discussed below, for *E. coli* mutagenesis in aging colonies (TADDEI *et al.* 1997), for ciprofloxacin (antibiotic)-induced resistance mutagenesis (CIRZ *et al.* 2005), and for mutagenesis conferring resistance to bile salts in Salmonella (PRIETO *et al.* 2006). The stringent response to amino-acid starvation is required for a transcription-associated mutagenesis in *E. coli* that targets stringent-response-controlled genes (WRIGHT *et al.* 1999) and for amino-acid-starvation-induced mutagenesis in *B. subtilis* (RUDNER *et al.* 1999). Two different stress responses to hypoxia in human cancer cells also increase mutagenesis. One does so by specific downregulation of mismatch-repair genes (MIHAYLOVA *et al.* 2003; KOSHIJI *et al.* 2005; BINDRA and GLAZER 2007). The other is postulated to promote genome rearrangement by its demonstrated downregulation of RAD51 and BRCA1 functions required for high-fidelity repair of DNA double-strand breaks (DSBs) (BINDRA *et al.* 2004). These stress responses exert temporal control or restriction of mutagenesis, which favors genomic stability when cells and organisms are well adapted to their environments (*i.e.*, not stressed) and increases mutagenesis, potentially accelerating evolution, specifically during stress when cells are maladapted to their environments. Except for the human examples, the ways by which the stress responses upregulate mutagenesis are mostly not understood. We focus here on how a stress response controls mutagenesis in an *E. coli* model system.

Stress-induced mutagenesis is perhaps best understood in the *E. coli* model system. A widely used assay system uses a +1 frameshift allele of a *lacIZ* fusion gene located in the F'128 plasmid in cells with a deletion of the chromosomal *lac* genes (CAIRNS and FOSTER 1991). When these cells are plated on lactose minimal medium, a few Lac⁺ revertant colonies are observed. Many of these arise from spontaneous generation-dependent mutations that occur during growth of the culture. Prolonged incubation of these plates results in the continuous accumulation of additional Lac⁺ revertants, which arise through two mechanisms, both different from the mechanisms that produce the generation-dependent mutants (reviewed by GALHARDO *et al.* 2007).

First, within the first few days, most of the Lac⁺ colonies are "point mutants" that possess a compensatory −1 frameshift mutation in the *lacIZ* gene (FOSTER and TRIMARCHI 1994; ROSENBERG *et al.* 1994). Cells that carry these mutations also carry increased numbers of secondary unselected mutations in other genomic regions, whereas most Lac⁻ cells starved on the same plates do not, indicating that a subpopulation of the cells undergoes genomewide hypermutation (TORKELSON *et al.* 1997; ROSCHE and FOSTER 1999; GODOY *et al.*

2000). Therefore, a subset of the starved cells experiences increased mutagenesis when compared with the majority of the cells. Hereafter we refer to this subpopulation as "hypermutable." This hypermutable cell subpopulation (HMS) appears to be important to the formation of most or all of the Lac⁺ stress-induced mutants (GONZALES *et al.* 2008). The hypermutable state is transient, ceasing after growth impairment is ended and growth resumes (LONGERICH *et al.* 1995; TORKELSON *et al.* 1997; ROSENBERG *et al.* 1998; ROSCHE and FOSTER 1999; GODOY *et al.* 2000).

Second, longer incubation also results in the formation of a significant proportion of *lac*-amplified colonies in which the leaky *lacIZ* allele is amplified to 20–50 tandem copies, which produce sufficient enzyme activity to allow growth on lactose (HASTINGS *et al.* 2000; POWELL and WARTELL 2001; KUGELBERG *et al.* 2006; SLACK *et al.* 2006). In summary, *E. coli* cells may either increase point-mutation rates or undergo extensive genomic rearrangement in response to a growth-limiting environment.

Both of these processes require induction of the general or starvation stress response controlled by RpoS (LOMBARDO *et al.* 2004). Point mutagenesis, but not amplification, also requires induction of the SOS DNA-damage stress response (CAIRNS and FOSTER 1991; McKENZIE *et al.* 2000, 2001). In this article, we focus on the role of the SOS response in the mechanism of stress-induced point mutagenesis. See HASTINGS (2007) for a review of the mechanisms of stress-induced amplification and genome rearrangement.

The molecular mechanism of point mutagenesis in the Lac system is now considerably well understood. It entails a switch from the normally high-fidelity DNA synthesis associated with recombination-dependent double-strand-break repair to an error-prone synthesis specifically under stress (PONDER *et al.* 2005). Several genetic requirements are known for stress-induced point mutagenesis, including DNA-recombination functions (HARRIS *et al.* 1994, 1996; FOSTER *et al.* 1996; HE *et al.* 2006) in addition to the genes required for induction of the SOS DNA-damage response (CAIRNS and FOSTER 1991; McKENZIE *et al.* 2000) and the σˢ (RpoS) general/starvation stress-response (LAYTON and FOSTER 2003; LOMBARDO *et al.* 2004) regulons, and the *dinB* gene encoding DNA polymerase (Pol) IV (McKENZIE *et al.* 2001).

DinB is the founding member of the most widespread subfamily of Y-family specialized DNA polymerases, with orthologs in bacteria, archaea, and eukaryotes, including humans (reviewed by NOHMI 2006). DinB/ Pol IV can perform high-fidelity translesion DNA synthesis (TLS) across a number of different DNA lesion substrates (JAROSZ *et al.* 2006; BJEDOV *et al.* 2007; YUAN *et al.* 2008). However, this enzyme shows a significant error rate when copying undamaged DNA templates (KOBAYASHI *et al.* 2002). Some mutations in DinB can abolish its TLS activity, without interfering with the

mutator phenotype caused by overexpression of DinB, suggesting that mutagenesis and TLS are independent activities of Pol IV (GODOY et al. 2007). Eighty-five percent of the stress-induced Lac$^+$ point mutations generated in the nongrowing cells arise in a DinB-dependent manner (MCKENZIE et al. 2001).

The dinB gene is under the control of the SOS response, which upregulates its transcription 10-fold (KIM et al. 2001). Additionally, the alternative σ (transcription) factor σ^s (RpoS), which is responsible for the general stress response, upregulates dinB expression transcriptionally by 2- to 3-fold upon entry into stationary phase (LAYTON and FOSTER 2003). Proteins such as Ppk (STUMPF and FOSTER 2005) and the chaperones GroEL (LAYTON and FOSTER 2005), RecA, and UmuD (GODOY et al. 2007) all seem to modulate DinB activity. An interesting in vivo role of DinB is SOS untargeted mutagenesis of phage λ (KIM et al. 1997). In it, −1 frameshift mutations in runs of G's are generated, similarly to the predominant mutations detected in the lac gene during stress-induced mutagenesis (FOSTER and TRIMARCHI 1994; ROSENBERG et al. 1994). On the other hand, DinB has no effect on the spontaneous mutation rate in growing cells (MCKENZIE et al. 2001, 2003; KUBAN et al. 2004; WOLFF et al. 2004). DinB is implicated as the DNA polymerase that, only during the stress responses, makes DSB-repair-associated errors that become stress-induced point mutations (PONDER et al. 2005).

The role of the SOS response in controlling mutagenesis in the Lac assay is a complex issue because several SOS-controlled genes are required for the process. dinB, recA, ruvA, and ruvB are all required for mutagenesis (CAIRNS and FOSTER 1991; HARRIS et al. 1994, 1996; FOSTER et al. 1996; MCKENZIE et al. 2001; HE et al. 2006) and are all upregulated by SOS (COURCELLE et al. 2001). Also, the F-encoded psiB gene exerts a negative effect on mutagenesis in SOS-derepressed cells (MCKENZIE et al. 2000) and is thought to inhibit SOS induction and RecA (reviewed by COX 2007). We sought to determine whether the requirement for induction of the SOS response in stress-induced mutagenesis reflects a need for upregulation solely of dinB or whether any other gene(s) is required at SOS-induced levels. We present evidence below that indicates, first, that DinB is the only SOS-controlled gene required at induced levels for efficient stress-induced point mutagenesis and, second, that, although SOS-induced levels of DinB are required, they are not sufficient to differentiate cells into a hypermutable condition.

MATERIALS AND METHODS

Bacterial strains, plasmids, and media: The bacterial strains used in this work are shown in Table 1. dinB(o^c) alleles were constructed as described below. Other strains were constructed using P1-mediated transduction as described (MILLER 1992).

The antibiotics used were as follows: ampicillin, 100 μg/ml; chloramphenicol, 25 μg/ml; tetracycline, 10 μg/ml; kanamycin, 30 μg/ml; and rifampicin, 40 μg/ml. 5-Bromo-4-chloro-3-indolyl-β-D-galactoside (X-gal) was used at 40 μg/mL. M9 minimal medium (MILLER 1992) was supplemented with 10 μg/ml of vitamin B1 and either 0.1% glycerol or 0.1% lactose. Luria–Bertani–Herskowitz (LBH) medium was used as described by TORKELSON et al. (1997).

The plasmids used in this study are listed in Table 2. Plasmids containing P$_{dinB}$lacZ fusions used in β-galactosidase assays for gene expression analysis were constructed by amplification of the dinB promoter (from bases −432 to −2 of dinB) with primers 5'-TCGGCTGAATTCTGTTCGA CTCGCTCGATAAT-3' and 5'-CGGTACAAGCTTGCTCACCT CTCAACACTGGT-3' and by cloning into the pFZY plasmid (KOOP et al. 1987) using the EcoRI and HindIII sites introduced in the primers. The dinB promoter was amplified from strain SMR4562 and cloned into pFZY to generate plasmid pPdinB and amplified from strains SMR10308 and SMR10309 to generate the plasmids pPdinBOC1 and pPdinBOC2, respectively.

Construction of the dinB(o^c) alleles and strains bearing them: We created each of two mutations predicted from previous work on other SOS genes (FRIEDBERG et al. 2005) to inactivate the predicted LexA-binding site in dinB (Figure 1A). The Lac assay strains carry two copies of dinB, one in the chromosome and one in F'128 (discussed in the RESULTS). The constructions required several steps as below. Primer sequences are given in the supporting information, File S1.

First, we linked the cat selectable marker with dinB. We chose to put a selectable marker in the lafU (formerly known as mbhA) gene, which is present immediately upstream from the 5'-end of dinB. The FRTcatFRT cassette was amplified from pKD3 (DATSENKO and WANNER 2000) using primers CatupdinB-F and CatupdinB-R. The product was used to obtain SMR4562 recombinants containing the lafU::FRTcatFRT insertion (allele ΔlafU2::FRTcatFRT), using short-homology recombination as described (DATSENKO and WANNER 2000). One recombinant containing the ΔlafU2::FRTcatFRT in the F' plasmid was selected. This strain (SMR10292) was used to amplify the ΔlafU2::FRTcatFRT-dinB$^+$ region by PCR using primers CatupdinB-F and dinBcatnock-R. This product was used as a template for PCR-mediated site-directed mutagenesis, altering the dinB promoter.

Next we constructed a ΔlafU-dinB deletion strain to be used as a recipient for allelic replacement with the site-directed dinB-mutant genes linked to ΔlafU2::FRTcatFRT. We created a FC36-derivative containing a deletion encompassing the 3' half of ΔlafU and the whole dinB gene using primers kandinBchrom-F and DinBRCAT to amplify FRTKanFRT from pKD13 (DATSENKO and WANNER 2000). The products were used for short-homology recombination in the FC36 background, creating strain SMR10299. A similar deletion in the same region in the F' plasmid was created by short-homology recombination in SMR4562, using FRTcatFRT amplified from pKD3 with primers CatupdinB-F and DinBRCAT. Location of the deletion in the F' plasmid was confirmed by the ability to conjugate the cat gene conferring chloramphenicol resistance. The cat gene was removed by FLP-mediated site-specific recombination using the pCP20 plasmid (DATSENKO and WANNER 2000). The resulting F'128 ΔlafU-dinB::FRT [allele Δ(lafU-dinB)2096(::FRT)] was mated into strain SMR10299, creating strain SMR10303 {SMR4562 Δ(lafU-dinB)2097(::FRT-KanFRT) [F' Δ(lafU-dinB)2096(::FRT)]}. This strain was used as a recipient for allelic replacement using the site-directed dinB mutants produced by PCR with the ΔlafU2::FRTcatFRT-dinB fragment as a template. The sequence of the promoter and coding sequence of the dinB gene from the Kan^R Cam^R recombinants was determined by PCR and DNA sequencing to